Pulsed magnetic field measurement system based on colossal magnetoresistance-B-scalar sensors for railgun investigation

T. Stankevič,[1,a)] L. Medišauskas,[1] V. Stankevič,[1] S. Balevičius,[1] N. Žurauskienė,[1] O. Liebfried,[2] and M. Schneider[2]
[1]*Center for Physical Sciences and Technology, Semiconductor Physics Institute, A. Goštauto Str. 11, LT-01108 Vilnius, Lithuania*
[2]*French-German Research Institute of Saint-Louis (ISL), 5, rue Général Cassagnou, F-68301 Saint-Louis, France*

(Received 8 February 2014; accepted 21 March 2014; published online 9 April 2014)

A high pulsed magnetic field measurement system based on the use of CMR-B-scalar sensors was developed for the investigations of the electrodynamic processes in electromagnetic launchers. The system consists of four independent modules (channels) which are controlled by a personal computer. Each channel is equipped with a CMR-B-scalar sensor connected to the measurement device—B-scalar meter. The system is able to measure the magnitude of pulsed magnetic fields from 0.3 T to 20 T in the range from DC up to 20 kHz independently of the magnetic field direction. The measurement equipment circuit is electrically separated from the ground and shielded against low and high frequency electromagnetic noise. The B-scalar meters can be operated in the presence of ambient pulsed magnetic fields with amplitudes up to 0.2 T and frequencies higher than 1 kHz. The recorded signals can be transmitted to a personal computer in a distance of 25 m by means of a fiber optic link. The system was tested using the electromagnetic railgun RAFIRA installed at the French-German Research Institute of Saint-Louis, France. © *2014 AIP Publishing LLC*. [http://dx.doi.org/10.1063/1.4870280]

I. INTRODUCTION

Electromagnetic launchers (EML) convert electrical energy into kinetic energy by application of Lorentz forces. In the simple case of the railgun, the propelling forces act on an armature which has to provide a sliding electrical contact between the rails. Recent developments focus on solid armature railguns which are able to accelerate massive projectiles to velocities of more than 2 km/s.[1,2] A solid armature is in general a metal work piece which has to conduct current amplitudes of several kA up to several MA. Thus one of the central technological challenges for the launchers of this type is the development of appropriate armatures. Due to the conventional skin effect, the proximity effect,[3] and the velocity skin effect[4] caused by the moving armature high current densities appear in the rear part of the sliding contact interface. This effect can induce phase transitions and exceptional wear of the armature and rail materials during the acceleration process. Therefore, quantitative information about the current distribution in the vicinity of the sliding contact interface is of greatest interest. The measurement of the magnetic field distribution is one of the methods to gather this information.[5] Corresponding measurement techniques need to have high spatial resolution and should be able to measure highly dynamic magnetic fields in the range of 0.1 kHz up to 20 kHz. Moreover, the operation of the electromagnetic (EM) railgun is accompanied by a powerful broadband electromagnetic radiation which induces large noise signals[6] in conventional measurement equipment. In the literature, this effect is often called electromagnetic interference (EMI). The greatest challenges are caused by low frequency (up to a few kHz) high amplitude magnetic field oscillations which penetrate deep through the shielding material and induce parasitic signals in the electrical circuits of the sensitive measurement devices.

It was demonstrated that the CMR-B-scalar sensors based on the colossal magnetoresistance (CMR) effect in thin manganite films can be successfully used to measure pulsed magnetic field distribution in the bore of a coilgun,[7] in the vicinity of railgun rails,[8] and inside them.[9] In this paper we present the design and the testing results of a new robust pulsed magnetic field measurement system which uses CMR-B-scalar magnetic field sensors and is intended for precise measurements at high EMI levels in the vicinity of high power railguns.

II. B-SCALAR MEASUREMENT SYSTEM

A. General setup

The B-scalar measurement system consists of four independent modules (channels)–B-scalar meters which are controlled by a personal computer (PC). Each channel is equipped with a CMR-B-scalar sensor connected by a custom-made twisted pair cable with a shielding sleeve. Four B-scalar meters can be connected using a duplex fiber optic data link to the hub which concentrates the signals and transmits them to the PC via the USB connection. Optionally, each B-scalar meter can be connected to the PC directly via USB, but the optical link ensures the galvanic separation and reliable long-range (25 m) data transmission to the PC. The measurement at each channel can be triggered separately by an electrical or an optical signal. Outside view pictures of B-scalar meters and the hub are shown in Fig. 1

a)E-mail: Tomas.Stankevic@fidi.lt

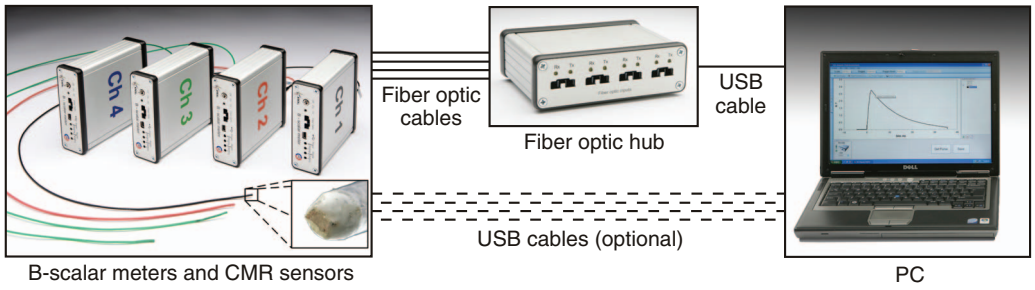

FIG. 1. The outside view and schematic diagram four-terminal pulsed magnetic field measurement system based on CMR-B-scalar sensors.

B. Magnetic field sensor

The sensor is based on the CMR effect exhibited by a thin manganite film deposited on a substrate with metal contacts deposited on it. The fabrication starts with the deposition of the 400 nm thick polycrystalline $La_{0.83}Sr_{0.17}MnO_3$ (LSMO) film on a lucalox substrate (99.9% Al_2O_3 + 0.1% MgO) using a MOCVD technique.[10] Next, by means of photo lithography and chemical etching the area of the film was reduced to 0.4×0.2 mm^2. Then, chromium and silver layers were thermally evaporated in a way that silver partly overlapped with the LSMO layer. Thus, an electric contact was created and the remaining part of the LSMO film defined the active volume of $400 \times 50 \times 0.40$ μm^3. Next, bifilarly twisted wires were soldered perpendicular to the surface of the film. The active area was then covered by hot melt adhesive material in order to protect the film from atmospheric conditions and to strengthen the solder joints. The twisted wire cable was additionally shielded against high frequency noise using a braided sleeve and covered with a flexible plastic tube. Finally, a connector was attached. The picture and schematic 3D cross section of the CMR-B-scalar sensor with cable are shown on Fig. 2.

C. B-scalar meter

The B-scalar meter is an electronic device developed specially for the measurements at the railgun. The main functional components of the B-scalar meter are shown in Fig. 3. The electronic circuits inside are protected against EMI by the enclosure consisting of an inner 4 mm thick steel box and an external 1.5 mm thick aluminum box. The thick steel enclosure is used to shield the electrical circuit against magnetic fields with frequencies down to 1 kHz. The lithium ion rechargeable battery (3.6 V) is used as power supply of the electronic circuits. It is mounted inside the steel enclosure and can be replaced by removing one of this enclosure walls. The internal power supply ensures that the device can be operated without being connected to any external power sources. The core of the device is the digital signal processor (DSP) Blackfin® 532 (Analog Devices), which operates at a clock rate of 400 MHz.

The measurement circuit was designed using a minimal number of analog components in order to minimize EMI. A constant stabilized 2.5 V DC voltage is applied to the sensor and a high thermal stability ballast resistor. The voltage signal from the sensor is buffered by a unity gain amplifier and filtered using a RC anti-aliasing filter. The signal is digitized using a 16 bit successive approximation analog-digital converter and transferred to the DSP via the Serial Peripheral Interface with 25 MHz maximum clock frequency. The maximum sampling rate was limited to 0.73 megasamples per second (MS/s) due to the duration of conversion and transfer of data. The use of a high resolution ADC allowed skipping the signal conditioning circuits, thus reducing the number of required analog components.

The B-scalar meter is set up through its communication line only. Thus, it uses a protocol based on text commands. All operations of the B-scalar meter are performed only on request of the external controlling program (PC software) and the trigger signal which initiates the measurement. However, each device can be regarded as self-sustaining, because when it enters the waiting state the signal can be measured even

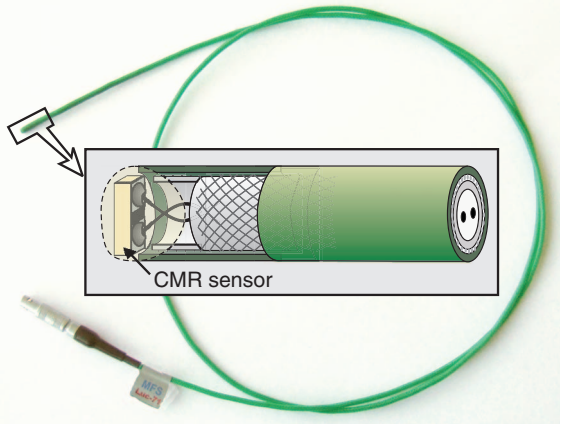

FIG. 2. Picture and schematic 3D cross section of the CMR-B-scalar sensor with cable (not to scale).

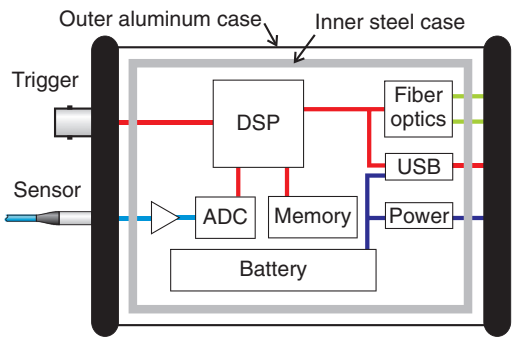

FIG. 3. Main functional blocks of the B-scalar meter.

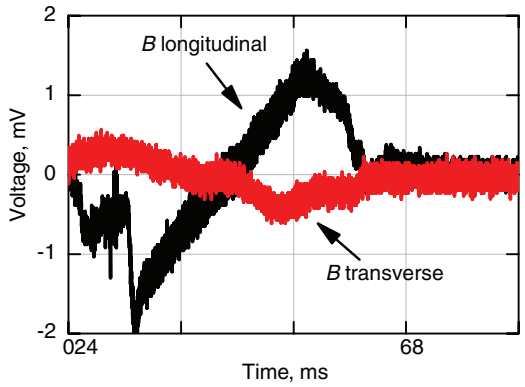

FIG. 4. EMI signals recorded by the B-scalar meter placed in the test coil in different orientations.

if the device is not connected to a PC. The protocol was designed to treat the connection or transfer errors adequately. It is crucial to ensure that every single measurement is successfully recorded and saved because a lot of resources are needed to prepare an experiment with a railgun.

The resistance of the B-scalar meter against the EMI was tested using a special setup consisting of a coil having 20 cm in diameter and a single pulse current generator. A magnetic pulse (duration of 5 ms) was generated and the signal was measured with the sensor being placed outside the coil. The voltage induced in the analog circuit of the B-scalar meter appeared in the measurement and as shown in Fig. 4 for two different orientations of the meter inside the coil. As it can be seen, the EMI amplitudes of the signal induced in the meter electronics are higher if the magnetic field is oriented along the long axis of the meter than for the perpendicular case. This is due to the numerous openings for the connectors at the front and rear panels.

The magnitude of the induced voltage was measured at different magnitudes and orientations of the device with respect to the magnetic field vector. The magnitude of the magnetic pulse was increased up to a threshold when the program running in the DSP stopped and a restart was required to continue. In conclusion we can state that the device is able to operate without significant signal distortions of the measured signal $<5\%$ at an ambient pulsed magnetic field with amplitudes up to 200 mT and frequencies of 200 Hz. It turned out that this allows for measurements at a distance of about 1 m from a high power railgun.

D. Fiber optic hub

The fiber optic hub is used for two purposes. The first is to convert optical signals back to electric signals; the second is to fuse data from four measurements into one USB channel. This is realized by using special integrated circuits which convert USB signals to four asynchronous serial data signals and vice versa in real time. Four data channels are connected to the optic transmitters and receivers. The fiber optic hub must be placed next to the PC at a safe distance (25 m) from the experiment site, since it is not protected against strong electromagnetic interference.

E. Software package

The software package developed for the B-scalar measurement system consists of firmware installed in the B-scalar meters and control software for the PC. The firmware is responsible for sampling the signal, storing the measured data, and sending it to the PC on demand. Thus it controls the hardware of the measurement device and implements a communication protocol. The firmware supports basic functions of a digital oscilloscope, such as adjusting the sampling frequency and choosing the trigger source and trigger level. The total number of data points remains equal 7300, whereas the length of the measured signal can be varied from 10 ms up to 5.12 s.

A measurement is set up by a click of a mouse button. Before starting the measurement the software checks whether each of the meters is connected to the sensor. When the measurement is set up each device enters the waiting state in which the data are constantly recorded to the buffer until the trigger signal initiates the start of the measurement. After the signal is sampled, it is additionally stored in the nonvolatile memory and can thus be later retrieved by the user via the control software. Additionally, a control sum is calculated which is used for the data transfer check. After the measurement, the data are automatically sent to the PC, processed according to the calibration data of each sensor and afterwards visualized on the screen as the $B(t)$ signal. Finally, the user has additional data management possibilities after the curves are acquired: renaming and saving the measured data in ASCII files, graph viewing tools (zoom, pan etc.). The user also has the possibility to update the firmware of the device using an additional piece of software supplied alongside the main program.

F. Calibration of the CMR sensors

The sensor's response is not a linear function of the magnetic flux density B. Moreover, it depends on temperature. Therefore, a calibration is necessary in order to assign a value of B to the magnetic field induced resistance change ΔR of the sensor. In order to increase the accuracy, the voltage change signal ΔV from the B-scalar meter was used instead of the values of the sensor's resistance change ΔR. The calibration was carried out using the high magnetic field generator described in Ref. 11. The CMR-B-scalar sensor and a reference B-dot sensor were placed in the center of the coil bore at approximately the same position. The B-dot sensor was calibrated in advance using a common search coil magnetometer based on Faraday's induction law. Discharging the capacitor bank through the coil, a half-sine shaped magnetic pulse of duration of 850 μs and amplitude of 25 T was generated. The signal of the CMR-B-scalar sensor was recorded by the B-scalar meter and transferred to the PC. At the same time the reference signal from the B-dot sensor was recorded by a digital oscilloscope. Then, the procedure is repeated in the temperature range 0–50 °C with a step of 3 °C. The temperature inside the coil was stabilized by an active temperature controlling system. The data recorded with both sensors were processed using MATLAB® routines to create the final calibration file.

It has to be noted that the total signal measured by the B-scalar meter is actually a superposition of three components

$U_s(t) = U_0 - \Delta U_{CMR}(t) + U_{loop}(t)$. Here U_0 is the initial voltage proportional to the resistance of the sensor at zero magnetic field. This voltage depends on the temperature of the sensor and it is considered to be constant during the duration of the pulse. $\Delta U_{CMR}(t) = f(|B|)$ is a voltage decrease due to the magnetoresistance effect. $U_{loop}(t)$ is a parasitic signal, caused by the so-called "loop effect"—a voltage induced in the sensor wires by the changing magnetic field. This effect was minimized using different techniques applied to both the sensor and the wiring.[12] As a result the influence of $U_{loop}(t)$ was negligible for pulses with frequencies up to 10 kHz.

Generally the calibration table is created by assigning the B values from the reference sensor to the ΔU values from the CMR-sensor signal measured at the same point in time: $B(t_i) \rightarrow \Delta U_{CMR}(t_i)$. The assignment $B(\Delta U)$ was made for each temperature (for each U_0) of calibration.

The anisotropic behavior of the sensors must also be taken into account since the orientation of the magnetic field during the experiment can be unknown or it can change in time. At low magnetic field amplitudes (up to ≈0.3 T) the sensor is more sensitive to the field component parallel to the active layer (LSMO film) than to that perpendicular to it.[13] During the calibration in the pulsed magnetic field the sensor is placed inside the coil in such a way that the active layer is perpendicular to the magnetic flux lines. A correction must be made to generate calibration data valid for the orientation range between the perpendicular and parallel case. The correction data are obtained from additional experiments performed in a constant magnetic field of a DC electromagnet for each temperature.

Finally, a family of calibration curves $B(\Delta U)$ for different U_0 (which correspond to different temperatures) fora particular CMR-B-scalar sensor are stored to PC. An example of such calibration curves is presented in Fig. 5.

III. EXPERIMENTAL RESULTS

The testing of the high magnetic field measurement system based on the array of CMR-B-Scalar sensors was performed using the railgun RApid FIre RAilgun (RAFIRA)[14] that was operated in single shot mode. The railgun RAFIRA with the CMR-B-scalar sensor setup is depicted in Fig. 6(a). The parameters of RAFIRA, its power supply, and the projectile used can be found in Ref. 14. Four CMR-B-scalar sensors were installed at the center of the railgun (white arrow in Fig. 6(b)) with the corresponding B-scalar meters placed below (white box in Fig. 6(b)), see also Refs. 8 and 9. Fig. 6(a) presents the sensor arrangement at the railgun in more details. Four sensors were mounted using a plastic block (not shown in drawing) at the side of the upper rail. Sensor S_1 measured magnetic field between the rails, whereas sensors S_2–S_4 measured magnetic fields as close as 0.5 mm from the surface of the rail.

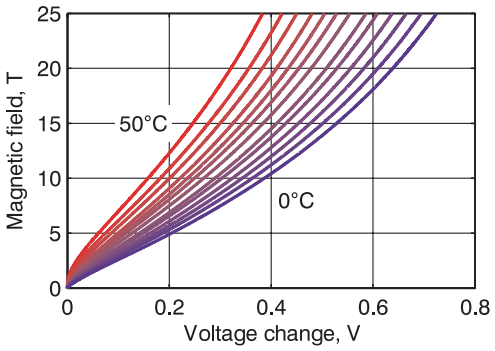

FIG. 5. Family of calibration curves for a particular CMR sensor.

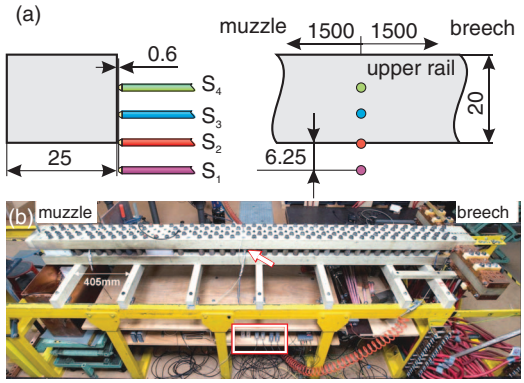

FIG. 6. Placement of the CMR-B-scalar sensors at the railgun RAFIRA (a). Outside view of the experimental setup. The position of the sensors is shown with a white arrow. The B-scalar meters are placed underneath, in the area marked with a white rectangle (b). The distances are given in millimeters.

A shot was performed using the projectile consisting of a sabot made of glass reinforced plastic and brush armatures. The total stored energy was 0.97 MJ. The velocity of the projectile measured using a Doppler radar was 1640 m/s at the sensor's position and 1780 m/s at the muzzle exit taking place at 3.1 ms. Further details concerning the sabot technology and brush armatures can be found in Refs. 8, 14, and 15.

Magnetic field versus time data deduced from each CMR sensor signal are shown in Fig. 7. First of all we can see that the magnetic field amplitude is zero up to $t = 2.1$ ms. Then, after the projectile passed the measurement position, the signal rapidly rises due to the magnetic field associated with the current distribution flowing along the upper rail. Just behind the projectile the current is confined to the inner part of the upper rail—a consequence of the velocity skin effect.[8,9] Pronounced maxima and large amplitudes of the measurements by the sensors S1 and S2 confirm that the largest current flows on the inner surface of the rail. The profiles obtained

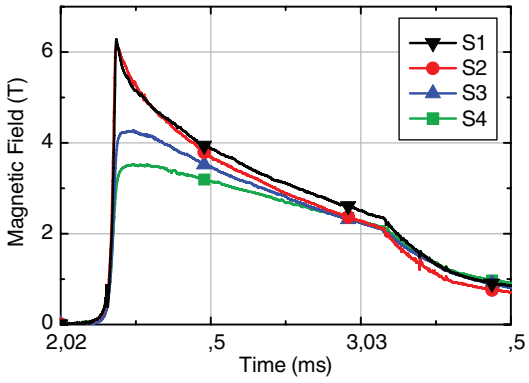

FIG. 7. Magnetic field measurements performed using the B-scalar measurement system during a railgun shot.

by sensors S3 and S4 are different though. Their maxima are much smaller and appear retarded in time. Both effects are to be expected, if the velocity-induced current concentrations at the inner rail surface and at the rear part of the armature occur, see, for instance, Fig. 2 in Ref. 2. After the passage of the projectile, the behavior of the magnetic field distribution is not only depending on the applied current pulse, but also follows the magnetic diffusion equation. The current pulse causes the general similarity between the different measurements, whereas magnetic diffusion is responsible for the individual differences.

IV. CONCLUSIONS

We have developed a pulsed magnetic field measurement system based on the CMR-B-scalar sensors for investigations of electrodynamic processes in electromagnetic launchers. The system is able to measure the magnitude of pulsed magnetic fields independently on their orientation in the range from 0.3 T to 25 T. It is protected against strong electromagnetic interference being typical for the dynamic operation of a high power railgun. The system can also be applied for the investigation of high pulsed magnetic fields in the frequency range up to 20 kHz generated by electromagnetic catapults[16] or small explosive magnetic generators.[17,18]

ACKNOWLEDGMENTS

This work was in part supported by the Research Council of Lithuania (Grant No. MIP-062/2012) and the French-Lithuanian Gilibert (Project No. TAP LZ 11/2013).

[1] M. Schneider and R. Schneider, IEEE Trans. Magn. **43**, 186 (2007).
[2] J. T. Tzeng and E. M. Schmidt, IEEE Trans. Plasma Sci. **39**, 149 (2011).
[3] S. L. M. Berleze and R. Robert, IEEE Trans. Educ. **46**, 368 (2003).
[4] G. C. Long and W. F. Weldon, IEEE Trans. Magn. **25**, 347 (1989).
[5] O. Liebfried, M. Schneider, and S. Balevicius, IEEE Trans. Plasma Sci. **39**, 431 (2011).
[6] G. Becherini, S. Di Fraia, G. Genovesi, A. Petri, S. Hundertmark, M. Schneider, and B. Tellini, IEEE Trans. Plasma Sci. **39**, 22 (2011).
[7] O. Liebfried, M. Loffler, M. Schneider, S. Balevičius, V. Stankevič, N. Žurauskienė, A. Abrutis, and V. Plausinaitiene, IEEE Trans. Magn. **45**, 5301 (2009).
[8] M. Schneider, O. Liebfried, V. Stankevič, S. Balevičius, and N. Žurauskienė, IEEE Trans. Magn. **45**, 430 (2009).
[9] T. Stankevič, M. Schneider, and S. Balevičius, IEEE Trans. Plasma Sci. **41**, 2790 (2013).
[10] N. Žurauskienė, S. Balevičius, P. Cimmperman, V. Stankevič, S. Keršulis, J. Novickij, A. Abrutis, and V. Plaušinaitienė, J. Low Temp. Phys. **159**, 64 (2009).
[11] J. Novickij, S. Balevičius, N. Žurauskienė, R. Kačianauskas, V. Stankevič, Č. Šimkevičius, S. Keršulis, and S. Bartkevičius, J. Low Temp. Phys. **159**, 406 (2009).
[12] S. Balevičius, V. Stankevič, N. Žurauskienė, Č. Šimkevičius, O. Liebfried, M. Löffler, M. Schneider, A. Abrutis, and V. Plaušinaitienė, Acta Phys. Pol., A **115**, 1133 (2009), http://przyrbwn.icm.edu.pl/APP/PDF/115/a115z661.pdf.
[13] N. Žurauskienė, S. Balevičius, V. Stankevič, S. Kersulis, M. Schneider, O. Liebfried, V. Plausinaitiene, and A. Abrutis, IEEE Trans. Plasma Sci. **39**, 411 (2011).
[14] M. Schneider, M. Woetzel, W. Wenning, and D. Walch, IEEE Trans. Magn. **45**, 442 (2009).
[15] M. Schneider, D. Eckenfels, and F. Hatterer, IEEE Trans. Magn. **39**, 76 (2003).
[16] G. Becherini, S. Di Fraia, and B. Tellini, IEEE Trans. Plasma Sci. **39**, 59 (2011).
[17] S. I. Shkuratov, E. F. Talantsev, J. Baird, M. F. Rose, Z. Shotts, L. L. Altgilbers, and A. H. Stults, Rev. Sci. Instrum. **77**, 043904 (2006).
[18] S. I. Shkuratov, E. F. Talantsev, J. Baird, M. F. Rose, Z. Shotts, Z. Roberts, L. L. Altgilbers, and A. H. Stults, IEEE Trans. Plasma Sci. **34**, 1866 (2006).